A R C H I V E O F M E C H A N I C A L E N G I N E E R I N G

VOL. LXV 2018 Number 2

DOI: 10.24425/123020

Key words: trigonometric plate theory, exponentially graded, elastic foundations

ASHRAF M. ZENKOUR[1,2]

TRIGONOMETRIC SOLUTION FOR AN EXPONENTIALLY GRADED THICK PLATE RESTING ON ELASTIC FOUNDATIONS

This article investigates the solution of exponentially graded (EG) thick rectangular plates resting on two-parameter elastic foundations according to a trigonometric plate theory (TPT). This theory includes the effect of both shear and normal strains thickness without needing to any shear correction factor. The displacement fields contains initial terms of a power series across plate thickness as well as additional trigonometric terms. The material properties of plate is graded such that Lamé's coefficients convert exponentially in a given constant orientation. Equilibrium equations according to the EG plate resting on Pasternak's foundations are derived. The solution is obtained by using Navier's technique. Numerical results for the EG thick plate on elastic foundations are presented, and compared with those available in the literature. The influences of Winkler's and Pasternak's parameters, side-to-thickness ratio, inhomogeneity parameter and aspect ratio on the bending responses of EG plates are investigated.

1. Introduction

The studies of plates resting on one- or two-parameter elastic foundations have drawn attention of a number of researchers [1–3]. They have enormous applications in structural engineering like swimming pools, buttress foundations and stockpiling tanks. It is well known that the simplest model for plate resting on elastic medium is known as Winkler's model. This model is deem a series of closely diverge, off and on independent, linear elastic vertical springs which, obviously, supply resistance in direct rate to the deflection of the plate [4]. The new model which is known as Pasternak's model has been amended Winkler's model by taking computation of the interactions between the separated springs and introducing a new dependent parameter [5].

[1] *Department of Mathematics, Faculty of Science, King Abdulaziz University, P.O. Box 80203, Jeddah 21589, Saudi Arabia. Email: zenkour@kau.edu.sa*

[2] *Department of Mathematics, Faculty of Science, Kafrelsheikh University, Kafrelsheikh 33516, Egypt. Email: zenkour@sci.kfs.edu.eg*

Functionally graded materials (FGMs) are advanced non-homogeneous composite materials that proposed for thermal barriers. They have increasingly applied for advanced engineering applications in extremely high temperature environment [6–8]. Three-dimensional (3D) solutions for FG plates are useful since they extend benchmark results to estimate the reliability of various two-dimensional (2D) plate theories and finite element formulations. In the 2D plate theory, many investigations with reference to problems of non-homogeneous plates have been published. A membrane identification has been presented in [9] to obtain an exact straightforward eigenvalues for buckling and vibration of FG plates resting on elastic foundation based on first-order shear deformation plate theory (FPT). The same membrane identification was later applied to the analyses of FG plates and shells based on a third-order plate theory [10, 11]. The free vibration, transient response, large deflection and post-buckling responses of FG thin plates resting on elastic foundations by using differential quadrature method and Galerkin's procedure have investigated in [12, 13]. A new hyperbolic shear and normal deformation plate theory has been presented in [14] to study the static, free vibration and buckling analysis of the simply-supported FG sandwich plates resting on elastic foundation. A simplified nth-higher-order theory with only two variables is introduced in [15] to study the free vibration of laminated plates. Recently, compressive studies for bending and free vibration of functionally graded plates and multilayered composite soft core sandwich plates resting on Winkler–Pasternak foundations have been investigated in [16, 17].

A new standard plate theory, that accounts for cosine shear stress distribution and free boundary conditions for shear stress upon the top and bottom surfaces of the plate, is firstly presented in [18]. This theory, also called trigonometric plate theory (TPT), corroborated and improved in [19]. The higher-order shear deformation plate theory (HPT) that neglects the transverse shear stresses on the plate faces has been proposed in [20]. The sinusoidal shear deformation plate theory (SPT) [21, 22] accounts according to a cosine-law distribution of transverse shear strains through the plate thickness. The present study involves the effects of both transverse normal and shear deformations by using the TPT. The 3D solution, the finite element method and the HPT are considered for the comparison purpose. The plate is presumed to be isotropic at any point in the plate volume moreover the plate resting on elastic foundations. The material properties of the plate like Lamé's coefficients varying exponentially through the plate thickness. The presented theory is revised for bending response of EG plate resting on Pasternak's foundations [23–25]. The stresses and displacements are extensive into series of trigonometric terms about the in-plane coordinates for a simply-supported plate, leading to a system of ordinary differential equations about the thickness coordinate, for which an exact solution is possible. The inclusion of the transverse normal stress is taken into consideration. Effects of various parameters on bending responses of EG plates are discussed. Numerical results are reported to serve as benchmarks for future comparison with other solutions.

2. Bending of the EG thick plate

2.1. Structural model

Consider an EG thick rectangular plate with the thickness h, length a, and width b, as shown in Fig. 1. The plate is resting on elastic foundation with Winkler's stiffness (K_W) and shear stiffness (K_P). The Cartesian coordinate system is established so that $0 \leqslant x \leqslant a$, $0 \leqslant y \leqslant b$ and $-h/2 \leqslant z \leqslant h/2$. Let the plate be subjected to a distributed transverse load $q(x, y)$ at the upper face ($z = +h/2$). Let the structure convert from the top to bottom surfaces according to an exponential law. So, the efficient material properties can be represented as:

$$\{\lambda, \mu\} = \{\lambda_0, \mu_0\} \mathrm{e}^{k\left(\frac{z}{h}+\frac{1}{2}\right)}, \tag{1}$$

in which λ_0 and μ_0 are Lamé's coefficients of the homogeneous plate,

$$\lambda_0 = \frac{\nu E}{(1+\nu)(1-2\nu)}, \qquad \mu_0 = \frac{E}{2(1+\nu)}, \tag{2}$$

and E and ν are Young's modulus and Poisson's ratio, respectively. It is to be noted that k ($k > 0$) is a parameter that transcribes the material variation profile through the plate thickness. The plate is perfectly homogeneous when k equals zero.

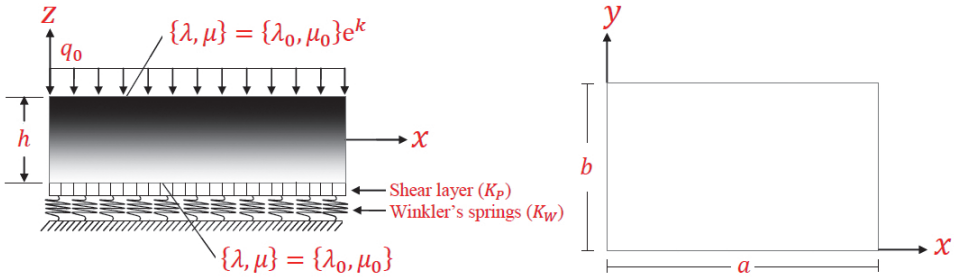

Fig. 1. Coordinate system and geometry of the EG thick rectangular plate resting on elastic foundations

2.2. Elastic foundation

Pasternak's model [1] is the most naturalistic amplification of the Winkler one. The reaction-deflection relation of shear layer and spring elements is expressed as:

$$E_f\Big|_{z=-h/2} = K_W w - K_P \left(\frac{\partial^2 w}{\partial x^2} + \frac{\partial^2 w}{\partial y^2}\right), \tag{3}$$

where E_f, w, K_W and K_P are the foundation reaction per unit area, deflection, and Winkler's and Pasternak's parameters, respectively. The present model is famous as the two-parameter Pasternak's foundations. This model is renowned as Winkler one when $K_P = 0$.

2.3. Displacement field

The trigonometric shear deformation plate theory (TPT) is suitable for the displacements [26]:

$$\begin{aligned} u_1(x,y,z) &= u(x,y) - z\frac{\partial w}{\partial x} + \Phi(z)\psi_1(x,y), \\ u_2(x,y,z) &= v(x,y) - z\frac{\partial w}{\partial y} + \Phi(z)\psi_2(x,y), \\ u_3(x,y,z) &= w(x,y) + \Phi'(z)\psi_3(x,y), \end{aligned} \tag{4}$$

where (u_1, u_2, u_3) are displacements of a general point (x, y, z) in EG plate, (u, v, w) are displacement projections on mid-plane and ψ_1 and ψ_2 are rotations about y- and x-axes, and ψ_3 is an additional undetermined function. The displacements u, v, w, ψ_1, ψ_2 and ψ_3 are functions of x and y, and $\Phi(z) = \dfrac{h}{\pi}\sin\left(\dfrac{\pi z}{h}\right)$. The prime $(')$ represents differentiation with respect to z. The effects of shear and normal deformation are both included. Note that the displacement field of FPT is given by $\Phi(z) = z$ and $\psi_3 = 0$. However, the displacement fields of HPT and SPT are given, respectively, by setting $\Phi(z) = z\left[1 - \dfrac{1}{3}\left(\dfrac{z}{h/2}\right)^2\right]$, $\psi_3 = 0$ and $\Phi(z) = \dfrac{h}{\pi}\sin\left(\dfrac{\pi z}{h}\right)$, $\psi_3 = 0$. The present theory comprise only one additional dependent unknown ($\psi_3 \neq 0$) than that of the remainder theories, but takes into consideration the effect of transverse normal strain through the plate thickness. No shear correction factor is needed for TPT, as well as for HPT and SPT. Now, the linear strains e_{ij} according to the displacements in Eq. (4), are presented as:

$$\begin{Bmatrix} e_{11} \\ e_{22} \\ e_{12} \end{Bmatrix} = \begin{Bmatrix} \varepsilon_{11} \\ \varepsilon_{22} \\ \varepsilon_{12} \end{Bmatrix} + z\begin{Bmatrix} \chi_{11} \\ \chi_{22} \\ \chi_{12} \end{Bmatrix} + \Phi(z)\begin{Bmatrix} \eta_{11} \\ \eta_{22} \\ \eta_{12} \end{Bmatrix}, \tag{5}$$

$$\{e_{13},\ e_{23}\} = \Phi'(z)\{\varepsilon_{13},\ \varepsilon_{23}\}, \qquad e_{33} = \Phi''(z)\varepsilon_{33}.$$

Here ε_{11}, χ_{ij} and η_{ij} are expressed as:

$$\begin{aligned} &\varepsilon_{11} = \frac{\partial u}{\partial x}, \quad \varepsilon_{22} = \frac{\partial v}{\partial y}, \quad \varepsilon_{33} = \psi_3, \quad \varepsilon_{12} = \frac{1}{2}\left(\frac{\partial v}{\partial x} + \frac{\partial x}{\partial y}\right), \\ &\{\varepsilon_{13},\ \varepsilon_{23}\} = \frac{1}{2}\left\{\psi_1 + \frac{\partial \psi_3}{\partial x},\ \psi_2 + \frac{\partial \psi_3}{\partial y}\right\}, \quad \chi_{11} = -\frac{\partial^2 w}{\partial x^2}, \quad \chi_{22} = -\frac{\partial^2 w}{\partial y^2}, \\ &\chi_{12} = -2\frac{\partial^2 w}{\partial x \partial y}, \quad \eta_{11} = \frac{\partial \psi_1}{\partial x}, \quad \eta_{22} = \frac{\partial \psi_2}{\partial y}, \quad \eta_{12} = \frac{1}{2}\left(\frac{\partial \psi_2}{\partial x} + \frac{\partial \psi_1}{\partial y}\right). \end{aligned} \tag{6}$$

2.4. Constitutive equations

The stress-strain relations for a linear isotropic elastic plate are represented as:

$$\sigma_{ij} = \lambda e_{kk}\delta_{ij} + 2\mu e_{ij}\,, \tag{7}$$

where δ_{ij} is the Kronecker's delta function. Also, the stress resultants may be defined as:

$$\begin{aligned} \left\{N_{ij}, M_{ij}, S_{ij}\right\} &= \int_{-h/2}^{+h/2} \{1, z, \Phi(z)\}\,\sigma_{ij}\mathrm{d}z, \qquad i,j = 1,2, \\ Q_{i3} &= \int_{-h/2}^{+h/2} \Phi'(z)\sigma_{i3}\mathrm{d}z, \qquad N_{33} = \int_{-h/2}^{+h/2} \Phi''(z)\sigma_{33}\mathrm{d}z. \end{aligned} \tag{8}$$

3. Equilibrium equations

Equations of equilibrium can be obtained due to the principle of virtual displacements. That is

$$\iint_{\Omega}\left[\int_{-h/2}^{h/2}\sigma_{ij}\delta e_{ij}\mathrm{d}z - (q - E_f)\delta w\right]\mathrm{d}\Omega = 0, \tag{9}$$

or

$$\begin{aligned} \iint_{\Omega}\Bigg[&N_{11}\frac{\partial\delta u}{\partial x} + N_{22}\frac{\partial\delta v}{\partial y} + N_{12}\left(\frac{\partial\delta u}{\partial y} + \frac{\partial\delta v}{\partial x}\right) + N_{33}\delta\psi_3 - M_{11}\frac{\partial^2\delta w}{\partial x^2} \\ &- M_{22}\frac{\partial^2\delta w}{\partial y^2} - 2M_{12}\frac{\partial^2\delta w}{\partial x\partial y} + S_{11}\frac{\partial\delta\psi_1}{\partial x} + S_{22}\frac{\partial\delta\psi_2}{\partial y} + S_{12}\left(\frac{\partial\delta\psi_2}{\partial x} + \frac{\partial\delta\psi_1}{\partial y}\right) \\ &+ Q_{13}\left(\delta\psi_1 + \frac{\partial\delta\psi_3}{\partial x}\right) + Q_{23}\left(\delta\psi_2 + \frac{\partial\delta\psi_3}{\partial y}\right) - (q - E_f)\delta w\Bigg]\mathrm{d}\Omega = 0. \end{aligned} \tag{10}$$

Then, by integrating by parts and setting the coefficients of δu, δv, δw, $\delta\psi_1$, $\delta\psi_2$ and $\delta\psi_3$ to zero, separately. So, according to TPT, we have

$$\begin{aligned} &\frac{\partial N_{11}}{\partial x} + \frac{\partial N_{12}}{\partial y} = 0, \qquad \frac{\partial N_{12}}{\partial x} + \frac{\partial N_{22}}{\partial y} = 0, \qquad \frac{\partial S_{11}}{\partial x} + \frac{\partial S_{12}}{\partial y} - Q_{13} = 0, \\ &\frac{\partial^2 M_{11}}{\partial x^2} + 2\frac{\partial^2 M_{12}}{\partial x\partial y} + \frac{\partial^2 M_{22}}{\partial y^2} + q - E_f = 0, \\ &\frac{\partial S_{12}}{\partial x} + \frac{\partial S_{22}}{\partial y} - Q_{23} = 0, \qquad \frac{\partial Q_{13}}{\partial x} + \frac{\partial Q_{23}}{\partial y} - N_{33} = 0. \end{aligned} \tag{11}$$

The stress resultants can be obtained in terms of total strains by substituting Eq. (7) into Eq. (8):

$$\begin{Bmatrix} N_{ij} \\ M_{ij} \\ S_{ij} \end{Bmatrix} = \begin{bmatrix} A_{11} & A_{12} & A_{13} \\ A_{12} & A_{22} & A_{23} \\ A_{13} & A_{23} & A_{33} \end{bmatrix} \begin{Bmatrix} \varepsilon_{ij} \\ \chi_{ij} \\ \eta_{ij} \end{Bmatrix} + \left(\begin{bmatrix} B_{11} & B_{12} & B_{13} \\ B_{12} & B_{22} & B_{23} \\ B_{13} & B_{23} & B_{33} \end{bmatrix} \begin{Bmatrix} \varepsilon_{11} + \varepsilon_{22} \\ \chi_{11} + \chi_{22} \\ \eta_{11} + \eta_{22} \end{Bmatrix} + \begin{Bmatrix} C_{11} \\ C_{12} \\ C_{13} \end{Bmatrix} \varepsilon_{33} \right) \delta_{ij},$$

$$N_{33} = D_{33}\varepsilon_{33} + [C_{11} \;\; C_{12} \;\; C_{13}] \begin{Bmatrix} \varepsilon_{11} + \varepsilon_{22} \\ \chi_{11} + \chi_{22} \\ \eta_{11} + \eta_{22} \end{Bmatrix}, \qquad Q_{i3} = D_{12}\varepsilon_{i3}, \tag{12}$$

where

$$\begin{aligned} \begin{Bmatrix} A_{l1} & A_{l2} & A_{l3} \\ B_{l1} & B_{l2} & B_{l3} \end{Bmatrix} &= \int_{-h/2}^{+h/2} \gamma \begin{Bmatrix} 2\mu(z) \\ \lambda(z) \end{Bmatrix} [1 \;\; z \;\; \Phi(z)] \mathrm{d}z, \\ C_{1l} &= \int_{-h/2}^{+h/2} \gamma\lambda(z)\Phi''(z)\mathrm{d}z, \\ D_{11} &= \int_{-h/2}^{+h/2} [\lambda(z) + 2\mu(z)][\Phi''(z)]^2 \mathrm{d}z, \\ D_{12} &= \int_{-h/2}^{+h/2} 2\mu(z)[\Phi'(z)]^2 \mathrm{d}z, \end{aligned} \tag{13}$$

in which $l = 1$ for $\gamma = 1$, $l = 2$ for $\gamma = z$, and $l = 3$ for $\gamma = \Phi(z)$. The substitution of Eq. (12) into Eq. (11) yields

$$[p]\{\delta\} = \{f\}, \tag{14}$$

in which $[p]$ is a symmetric matrix of differential operators and $f = \{0, 0, -q, 0, 0, 0\}^t$ is a generalized force vector while $\{\delta\} = \{u, v, w, \psi_1, \psi_2, \psi_3\}^t$. The elements $p_{ij} = p_{ji}$ of the symmetric matrix $[p]$ are given in Appendix A.

4. Two-dimensional solution

The following simply-supported boundary conditions are enjoined at the side edges of the present EG plate:

$$\begin{aligned} v = w = \psi_2 = \psi_3 = N_{11} = M_{11} = S_{11} = 0 \quad \text{at} \quad x = 0, a, \\ u = w = \psi_1 = \psi_3 = N_{22} = M_{22} = S_{22} = 0 \quad \text{at} \quad y = 0, b. \end{aligned} \tag{15}$$

Navier presented the external force as

$$q(x,y) = \sum_{m=1}^{\infty}\sum_{n=1}^{\infty} q_{mn}\sin(\alpha_m x)\sin(\beta_n y), \tag{16}$$

where $\alpha_m = m\pi/a$, $\beta_n = n\pi/b$; m and n are mode numbers. For uniformly distributed load (UDL), q_{mn} are expressed as:

$$q_{mn} = \begin{cases} \dfrac{16q_0}{mn\pi^2} & \text{for odd } m \text{ and } n, \\ 0 & \text{otherwise,} \end{cases} \tag{17}$$

where q_0 represents the load intensity at the plate centre. However, $m = n = 1$ and $q_{11} = q_0$ for sinusoidally distributed load (SDL). Following Navier's procedure, we suppose that

$$\begin{Bmatrix} (u,\psi_1) \\ (w,\psi_3) \\ (v,\psi_2) \end{Bmatrix} = \sum_{m=1}^{\infty}\sum_{n=1}^{\infty} \begin{Bmatrix} (U_{mn},X_{mn})\cos(\alpha_m x)\sin(\beta_n y) \\ (W_{mn},Z_{mn})\sin(\alpha_m x)\sin(\beta_n y) \\ (V_{mn},Y_{mn})\sin(\alpha_m x)\cos(\beta_n y) \end{Bmatrix}, \tag{18}$$

where U_{mn}, V_{mn}, W_{mn}, X_{mn}, Y_{mn} and Z_{mn} are arbitrary parameters. Eq. (14) in conjunction with Eq. (18) can be combined into a system of first-order equations as:

$$[P]\{\Delta\} = \{F\}, \tag{19}$$

where $\{\Delta\}$ and $\{F\}$ denote the columns:

$$\begin{aligned} \{\Delta\} &= \{U_{mn}, V_{mn}, W_{mn}, X_{mn}, Y_{mn}, Z_{mn}\}^t, \\ \{F\} &= \{0, 0, -q_{mn}, 0, 0, 0\}^t, \end{aligned} \tag{20}$$

and the elements $P_{ij} = P_{ji}$ of the coefficient matrix $[P]$ are reported in Appendix B.

5. Numerical results and discussions

Bending response of simply-supported EG thick rectangular plates resting on Pasternak's foundations and under SDL/UDL is investigated. The dimensionless deflection and stresses given here are presented as:

$$\begin{gathered} \bar{w} = \frac{10Eh^3}{a^4 q_0} w, \quad \kappa_W = \frac{a^4}{Eh^3} K_W, \quad \kappa_P = \frac{a^2}{Eh^3} K_P, \\ \{\sigma_1, \sigma_2, \sigma_6\} = \frac{10h^2}{a^2 q_0}\{\sigma_{11}, \sigma_{22}, \sigma_{12}\}, \quad \{\sigma_4, \sigma_5\} = \frac{10h}{aq_0}\{\sigma_{23}, \sigma_{13}\}, \\ \sigma_3 = -\frac{10^2 h^2}{a^2 q_0}\sigma_{33}, \quad \kappa_W^* = \frac{a^4}{D} K_W, \quad \kappa_P^* = \frac{a^2}{D} K_P, \quad D = \frac{Eh^3}{12(1-\nu^2)}. \end{gathered} \tag{21}$$

The results for EG thick rectangular plates resting on Pasternak's foundations using TPT are discussed for various values of aspect ratios a/b, side-to-thickness a/h, inhomogeneity parameter k and foundation parameters κ_W and κ_P. The results are documented in Tables 1–4 as well as in Figs. 2–6. For the sake of completeness and comparison, some results obtained using HPT and SPT are also presented in Table 3. It is assumed in all of the analysed cases (unless otherwise stated) that $a = 4h$, $b = 3a$, $k = 1.5$, and $\nu = 0.3$.

Numerical results for bending of homogeneous plates resting on Pasternak's foundations using TPT are compared with the corresponding ones available in the literature [27–31]. The plate is assumed to be subjected to UDL on the upper face and the deflections of the plate are given in Tables 1 and 2. The effects of foundation stiffness, loadings, and gradient index on the mechanical behaviour of EG plate will be intensively discussed. The results in Tables 1 and 2 are obtained by taking fifty-one terms in Eq. (14) and found to agree well with that reported in [27–31].

Table 1 contains the deflection $\hat{w} = \dfrac{10^3 D}{a^4 q_0} w\left(\dfrac{a}{2}, \dfrac{b}{2}, \dfrac{h}{2}\right)$ due to a UDL homogeneous square plate resting on elastic foundations ($h = 0.01a$). The present results are compared with those of 3D solution [30]. Also, the deflections presented in Table 1 using TPT agree extremely well with those obtained in [28] and [31]. It is clear that the deflection decreases as the elastic foundation parameters increase.

Table 1.

Comparisons of the deflections $\hat{w}$ of UDL homogeneous square plate ($h/a = 0.01$) on Winkler–Pasternak foundations

κ_W^*	κ_P^*	Present	Ref. [28]	Ref. [30]	Ref. [31]
1	1	3.84259	3.853	3.8546	3.855
	3^4	0.76253	0.763	0.7630	0.763
	5^4	0.11529	0.115	0.1153	0.1153
3^4	1	3.20219	3.210	3.2105	3.2108
	3^4	0.73133	0.732	0.7317	0.7317
	5^4	0.11452	0.115	0.1145	0.1145
5^4	1	1.47484	1.476	1.4765	1.4765
	3^4	0.57014	0.570	0.5704	0.5704
	5^4	0.10946	0.109	0.1095	0.1095

Table 2 gives a comparison of the central deflection $\breve{w} = \dfrac{10^2 D}{a^4 q_0} w\left(\dfrac{a}{2}, \dfrac{b}{2}, 0\right)$ of an isotropic square plate on one-parameter elastic foundation under UDL. It is obvious that TPT gives results that compared well with the available ones [27, 29]. In addition, the deflection decreases as Winkler's parameter κ_W^* increases.

Table 2.

Comparisons of the central deflections $\breve{w}$ of UDL homogeneous square plate on Winkler's foundations ($h/a = 0.05$)

κ_W^*	Present	Ref. [29]	Ref. [27]
0	0.40958	0.40624	0.41197
1^4	0.40850	0.40517	0.41088
3^4	0.33702	0.33472	0.33855
5^4	0.15099	0.15060	0.15114
10^4	0.01110	0.01115	0.01096

Table 3 gives the effect of inhomogeneity parameter k and side-to-thickness ratio a/h on the deflection $\bar{w}$ of EG thick rectangular plates resting on Pasternak's foundations. Also, the deflection $\bar{w}$ decreases as all of the parameters κ_W, κ_P, k and a/h increase.

Table 3.

Effects of inhomogeneity parameter k and side-to-thickness ratio a/h on the defection $\bar{w}(0)$ of EG thick rectangular plate resting on elastic foundations

k	κ_W	κ_P	$a = 3h$			$a = 5h$		
			TPT	HPT	SPT	TPT	HPT	SPT
0.1	0	0	1.12265	0.99049	1.00350	0.95629	0.81134	0.81299
	10	0	0.53933	0.49761	0.50087	0.49354	0.44792	0.44843
	10	10	0.08052	0.07707	0.07714	0.07826	0.07576	0.07578
0.3	0	0	1.01508	0.90859	0.90789	0.86475	0.73604	0.73586
	10	0	0.51315	0.47605	0.47586	0.46795	0.42398	0.42392
	10	10	0.07989	0.07653	0.07652	0.07758	0.07505	0.07505
0.5	0	0	0.91715	0.82189	0.82130	0.78150	0.66640	0.66625
	10	0	0.48679	0.45112	0.45094	0.44241	0.39990	0.39985
	10	10	0.07921	0.07586	0.07585	0.07683	0.07426	0.07425
0.8	0	0	0.78665	0.70692	0.70647	0.67068	0.57439	0.57429
	10	0	0.44722	0.41415	0.41399	0.40449	0.36484	0.36479
	10	10	0.07803	0.07473	0.07473	0.07557	0.07295	0.07295
1.0	0	0	0.70954	0.63920	0.63884	0.60527	0.52038	0.52030
	10	0	0.42107	0.38995	0.38981	0.37968	0.34227	0.34224
	10	10	0.07714	0.07391	0.07390	0.07463	0.07201	0.07200
1.5	0	0	0.54675	0.49647	0.49632	0.46737	0.40682	0.40680
	10	0	0.35753	0.33176	0.33169	0.32025	0.28912	0.28917
	10	10	0.07456	0.07153	0.07153	0.07193	0.06933	0.06933

Fig. 2a displays the effect of elastic foundations on the variation of $\bar{w}$ versus side-to-thickness ratio a/h of EG square plate. The deflection $\bar{w}$ decreases as Pasternak's foundation parameters increase. For higher values of elastic founda-

tion parameters, the deflection may be independent of a/h ratio. Fig. 2b gives the variation of $\bar{w}$ versus aspect ratio a/b of EG rectangular plate resting on elastic foundations. The deflection $\bar{w}$ decreases as ratio a/b and elastic foundation parameters increase. It is clear that TPT gives deflection closes to that of HPT for plates subjected to Pasternak's model.

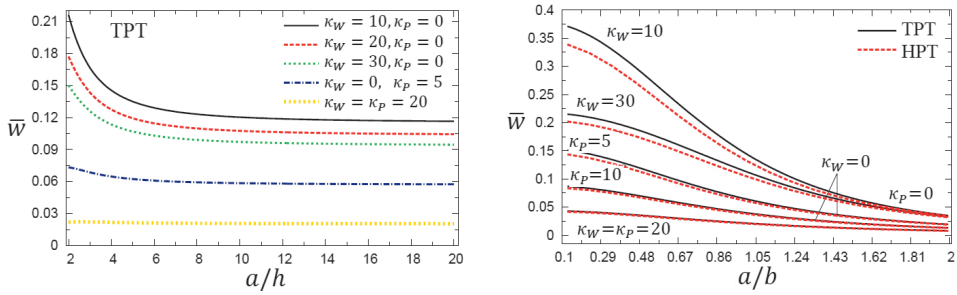

(a) $\bar{w}$ vs a/h $(a = b)$ (b) $\bar{w}$ vs a/b

Fig. 2. Variation of $\bar{w}$ of the EG plate resting on elastic foundations $(z = 0)$

Fig. 3a shows that the effect of thickness on $\bar{w}$ of EG thick square plate resting on Pasternak's foundations. It is clear that the deflection decreases as the parameters κ_W and κ_P increase. Fig. 3b shows the effect of elastic foundations on σ_1 through-the-thickness of EG thick rectangular plate. The tensile stress σ_1 decreases with the increase of elastic foundations κ_W and κ_P while the compressive stress σ_1 increases. It is clear that the tensile stress σ_1 is vanished above the mid-surface of the plate.

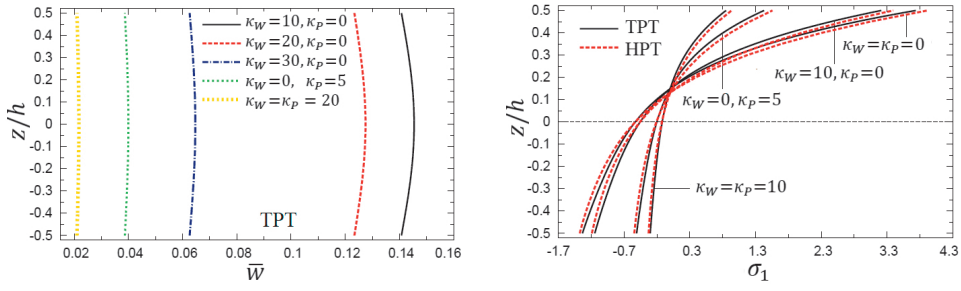

(a) The deflection $\bar{w}$ using TPT (b) The stress σ_1 using TPT and HPT

Fig. 3. Through-the-thickness distributions of $\bar{w}$ and σ_1 of the EG square plate resting on elastic foundations

Table 4 displays the effect of inhomogeneity parameter k on stresses of EG thick rectangular plate resting on elastic foundations by using TPT. It is shown that σ_1, σ_2 and σ_3 decrease rapidly as κ_W and κ_P increase whereas they increase by increasing the parameter k. The transverse shear stresses σ_4 and σ_5 as well as the

Table 4.

Effect of the inhomogeneity parameter k on the stresses of the EG thick rectangular plate resting on elastic foundations by TPT

k	κ_W	κ_P	Stresses					
			σ_1	σ_2	σ_3	σ_4	σ_5	σ_6
0.1	0	0	5.66146	2.49307	0.39077	1.46947	4.40842	2.34754
	10	0	2.85625	1.25777	0.19715	0.74136	2.22408	1.18435
	10	10	0.44395	0.19549	0.03064	0.11523	0.34569	0.18409
0.3	0	0	6.05954	2.65626	1.17144	1.46707	4.40122	2.14999
	10	0	3.20915	1.40676	0.62039	0.77697	2.33089	1.13864
	10	10	0.52109	0.22843	0.10074	0.12616	0.37849	0.18489
0.5	0	0	6.48186	2.83066	1.94947	1.46228	4.38684	1.96779
	10	0	3.59534	1.57010	1.08132	0.81109	2.43328	1.09149
	10	10	0.61109	0.26686	0.18379	0.13786	0.41358	0.18552
0.8	0	0	7.16399	3.11568	3.10767	1.45067	4.35202	1.72099
	10	0	4.24077	1.84434	1.83961	0.85873	2.57620	1.01875
	10	10	0.77461	0.33688	0.33602	0.15686	0.47057	0.18608
1.0	0	0	7.65347	3.32298	3.87129	1.44004	4.32012	1.57271
	10	0	4.71759	2.04828	2.38626	0.88764	2.66292	0.96942
	10	10	0.90607	0.39339	0.45831	0.17048	0.51144	0.18619
1.5	0	0	9.01139	3.91064	5.73722	1.40376	4.21127	1.25234
	10	0	6.08431	2.64039	3.87365	0.94779	2.84337	0.84556
	10	10	1.33368	0.57877	0.84910	0.20775	0.62326	0.18535

in-plane tangential stress σ_6 are decreasing with the increase of foundation and inhomogeneity parameters.

Fig. 4(a, b) show, respectively, the effect of elastic foundations on stresses σ_6 and σ_3 through-the-thickness of EG thick rectangular plate. The in-plane stress σ_6 may be vanished at $z/h = 0.05$. The tensile stress σ_6 increases with the increase of elastic foundations κ_W and κ_P while the compressive stress σ_6 decreases. The normal stress σ_3 may be vanished at $z/h = 0.4$. The tensile stress σ_3 increases with the increase of elastic foundations κ_W and κ_P while the compressive stress decreases. The minimum value of compressive stress σ_3 occurs at the top surface of plate without elastic foundation. However, the maximum value of the tensile stress σ_3 occurs at the lower face of plate without elastic foundation.

Fig. 5(a, b) plots the through-the-thickness distributions of transverse shear stresses σ_4 and σ_5 of EG thick square plate resting on elastic foundations. The transverse shear stresses σ_4 and σ_5 are decreasing as the increase of κ_W and κ_P. Also the stresses σ_4 and σ_5 are maximum when z/h takes positive values above the mid-plane of the plate. However, the stresses are maximum for plates without

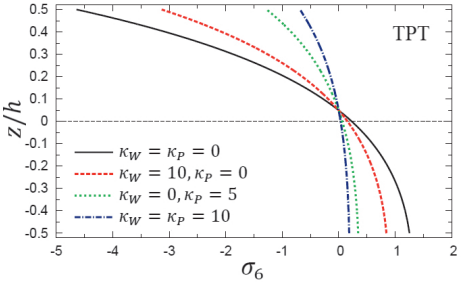

(a) The stress σ_6 using TPT

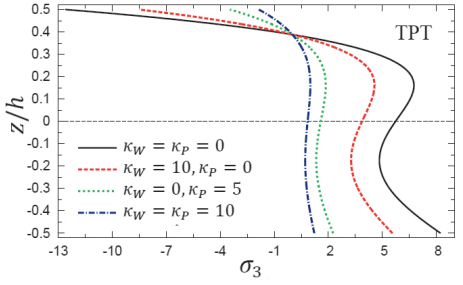

(b) The stress σ_3 using TPT

Fig. 4. Through-the-thickness distributions of σ_6 and σ_3 of the EG plate on elastic foundations

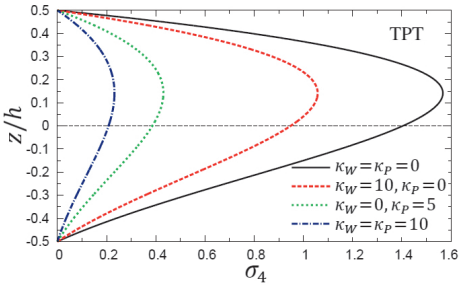

(a) Transverse shear stress σ_4

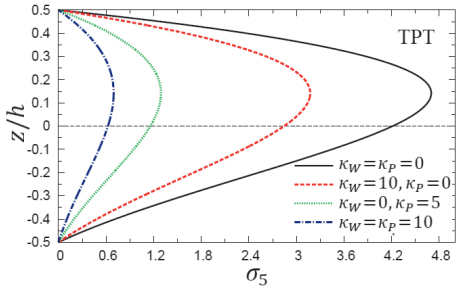

(b) Transverse shear stress σ_5

Fig. 5. Through-the-thickness distributions of σ_4 and σ_5 of the EG plate on elastic foundations

elastic foundations but they are minimum when elastic foundations are taken into account.

Finally, in Fig. 6(a, b) the through-the-thickness distributions of transverse shear stresses σ_4 and σ_5 of EG thick square plate resting on Pasternak's foundations are plotted for different values of inhomogeneity parameter k. One can observe that

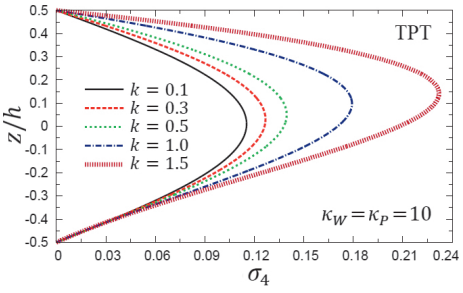

(a) Transverse shear stress σ_4

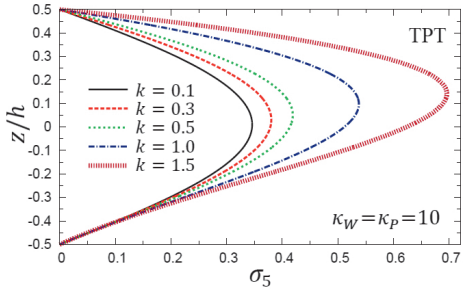

(b) Transverse shear stress σ_5

Fig. 6. Through-the-thickness distributions of σ_4 and σ_5 of the EG plate resting on Pasternak's foundations

σ_4 and σ_5 are increasing by increasing the parameter k. As seen from Fig. 6, the maximum values of σ_4 and σ_5 do not occur at $z/h = 0$. They occur at points a little above the mid-plane of EG plate. In addition, the shear stresses are affected strongly by the exponentially graded parameter k.

6. Conclusions

The bending responses of exponentially graded thick rectangular plates resting on Pasternak's foundations are described and discussed using TPT. The interaction between the plate and elastic foundations is included in formulations. Results corresponding to different parameters k, a/h, a/b, κ_W and κ_P are investigated. In general, the trigonometric solution provides benchmark results, that can be used for the evaluation of different plate theories and also to compare with results obtained by other exact solution, approximate methods such as the finite-element method and analytical solutions. The present TPT does not need any shear correction factors. Convergence and comparison studies show the accuracy and numerical stability of this theory. The numerical results given here represent a point of reference for the analysis of the EG thick plates on elastic foundations. For thick EG plates, the present trigonometric theory predicts displacements and stresses more accuracy when compared to other higher-order shear deformation plate theory.

Appendices

Apendix A

The elements of the symmetric matrix $[p]$ presented in Eq. (12) are given by

$$p_{11} = (A_{11} + B_{11})\frac{\partial^2}{\partial x^2} + \frac{1}{2}A_{11}\frac{\partial^2}{\partial y^2}, \quad p_{12} = \left(\frac{1}{2}A_{11} + B_{11}\right)\frac{\partial^2}{\partial x \partial y},$$

$$p_{13} = -(A_{12} + B_{12})\left(\frac{\partial^3}{\partial x^3} + \frac{\partial^3}{\partial x \partial y^2}\right), \quad p_{14} = (A_{13} + B_{13})\frac{\partial^2}{\partial x^2} + \frac{1}{2}A_{13}\frac{\partial^2}{\partial y^2},$$

$$p_{15} = \left(\frac{1}{2}A_{13} + B_{13}\right)\frac{\partial^2}{\partial x \partial y}, \quad p_{16} = C_{11}\frac{\partial}{\partial x},$$

$$p_{22} = (A_{11} + B_{11})\frac{\partial^2}{\partial y^2} + \frac{1}{2}A_{11}\frac{\partial^2}{\partial x^2}, \quad p_{23} = -(A_{12} + B_{12})\left(\frac{\partial^3}{\partial x^2 \partial y} + \frac{\partial^3}{\partial y^3}\right),$$

$$p_{24} = p_{15}, \quad p_{25} = (A_{13} + B_{13})\frac{\partial^2}{\partial y^2} + \frac{1}{2}A_{13}\frac{\partial^2}{\partial x^2}, \quad p_{26} = C_{11}\frac{\partial}{\partial y},$$

$$p_{33} = -(A_{22} + B_{22})\left(\frac{\partial^2}{\partial x^2} + \frac{\partial^2}{\partial y^2}\right)^2 - K_W + K_P\left(\frac{\partial^2}{\partial x^2} + \frac{\partial^2}{\partial y^2}\right),$$

$$p_{34} = (A_{23} + B_{23})\left(\frac{\partial^3}{\partial x^3} + \frac{\partial^3}{\partial x \partial y^2}\right),$$

$$p_{35} = (A_{23} + B_{23})\left(\frac{\partial^3}{\partial x^2 \partial y} + \frac{\partial^3}{\partial y^3}\right), \quad p_{36} = -C_{12}\left(\frac{\partial^2}{\partial x^2} + \frac{\partial^2}{\partial y^2}\right),$$

$$p_{44} = (A_{33} + B_{33})\frac{\partial^2}{\partial x^2} + \frac{1}{2}A_{33}\frac{\partial^2}{\partial y^2} - \frac{1}{2}D_{12}, \quad p_{45} = \left(\frac{1}{2}A_{33} + B_{33}\right)\frac{\partial^2}{\partial x \partial y},$$

$$p_{46} = \left(C_{13} - \frac{1}{2}D_{12}\right)\frac{\partial}{\partial x}, \quad p_{55} = (A_{33} + B_{33})\frac{\partial^2}{\partial y^2} + \frac{1}{2}A_{33}\frac{\partial^2}{\partial x^2} - \frac{1}{2}D_{12},$$

$$p_{56} = \left(C_{13} - \frac{1}{2}D_{12}\right)\frac{\partial}{\partial y}, \quad p_{66} = D_{11} - \frac{1}{2}D_{12}\left(\frac{\partial^2}{\partial x^2} + \frac{\partial^2}{\partial y^2}\right).$$

Apendix B

The elements of the symmetric matrix $[P]$ presented in Eq. (17) are given by

$$P_{11} = -\alpha_m^2(A_{11} + B_{11}) - \frac{1}{2}\beta_n^2 A_{11}\frac{\partial^2}{\partial y^2}, \quad P_{12} = -\alpha_m\beta_n\left(\frac{1}{2}A_{11} + B_{11}\right),$$

$$P_{13} = \alpha_m(\alpha_m^2 + \beta_n^2)(A_{12} + B_{12}), \quad P_{14} = -\alpha_m^2(A_{13} + B_{13}) - \frac{1}{2}\beta_n^2 A_{13},$$

$$P_{15} = -\alpha_m\beta_n\left(\frac{1}{2}A_{13} + B_{13}\right), \quad P_{16} = \alpha_m C_{11},$$

$$P_{22} = -\beta_n^2(A_{11} + B_{11}) - \frac{1}{2}\alpha_m^2 A_{11}, \quad P_{23} = \beta_n(\alpha_m^2 + \beta_n^2)(A_{12} + B_{12}),$$

$$P_{24} = P_{15}, \quad P_{25} = -\beta_n^2(A_{13} + B_{13}) - \frac{1}{2}\alpha_m^2 A_{13}, \quad P_{26} = \beta_n C_{11},$$

$$P_{33} = -(\alpha_m^2 + \beta_n^2)^2(A_{22} + B_{22}) - K_W - K_P(\alpha_m^2 + \beta_n^2),$$

$$P_{34} = \alpha_m(\alpha_m^2 + \beta_n^2)(A_{23} + B_{23}),$$

$$P_{35} = \beta_n(\alpha_m^2 + \beta_n^2)(A_{23} + B_{23}), \quad P_{36} = -(\alpha_m^2 + \beta_n^2)C_{12},$$

$$P_{44} = -\alpha_m^2(A_{33} + B_{33}) - \frac{1}{2}\beta_n^2 A_{33} - \frac{1}{2}D_{12}, \quad P_{45} = -\alpha_m\beta_n\left(\frac{1}{2}A_{33} + B_{33}\right),$$

$$P_{46} = \alpha_m\left(C_{13} - \frac{1}{2}D_{12}\right), \quad P_{55} = -\beta_n^2(A_{33} + B_{33}) - \frac{1}{2}\alpha_m^2 A_{33} - \frac{1}{2}D_{12},$$

$$P_{56} = \beta_n\left(C_{13} - \frac{1}{2}D_{12}\right), \quad P_{66} = -D_{11} - \frac{1}{2}(\alpha_m^2 + \beta_n^2)D_{12}.$$

Manuscript received by Editorial Board, December 28, 2017;
final version, April 04, 2018.

References

[1] X.-L. Huang and J.-J. Zheng. Nonlinear vibration and dynamic response of simply supported shear deformable laminated plates on elastic foundations. *Engineering Structures*, 25(8):1107–1119, 2003. doi: 10.1016/S0141-0296(03)00064-6.

[2] P. Malekzadeh and A.R. Setoodeh. Large deformation analysis of moderately thick laminated plates on nonlinear elastic foundations by DQM. *Composite Structures*, 80(4):569–579, 2007. doi: 10.1016/ j.compstruct.2006.07.004.

[3] P.H. Wen. The fundamental solution of Mindlin plates resting on an elastic foundation in the Laplace domain and its applications. *International Journal of Solids and Structures*, 45(3–4):1032–1050, 2008. doi: 10.1016/j.ijsolstr.2007.09.020.

[4] A.M. Zenkour. A comparative study for bending of cross-ply laminated plates resting on elastic foundations. *Smart Structures and Systems*, 15(6):1569–1582, 2015. doi: 10.12989/sss.2015.15.6.156.

[5] P.L. Pasternak. On a new method of analysis of an elastic foundation by means of two foundation constants. Gosudarstvennoe Izdatelstvo Literaturi po Stroitelstvu i Arkhitekture, Moscow, 1–56, 1954.

[6] J.N. Reddy. Analysis of functionally graded plates. *International Journal of Numerical Methods in Engineering*, 47(1–3):663–684, 2000. doi: 10.1002/(SICI)1097-0207(20000110/30)47:1/3<663::AID-NME787>3.0.CO;2-8.

[7] S.S. Vel and R.C. Batra. Exact solution for thermoelastic deformations of functionally graded thick rectangular plates. *AIAA Journal*, 40(7):1421–1433, 2002. doi: 10.2514/2.1805.

[8] S.A. Al Khateeb and A.M. Zenkour. A refined four-unknown plate theory for advanced plates resting on elastic foundations in hygrothermal environment. *Composite Structures*, 111:240–248, 2014. doi: 10.1016/j.compstruct.2013.12.033.

[9] Z.Q. Cheng and S. Kitipornchai. Membrane analogy of buckling and vibration of inhomogeneous plates. *Journal of Engineering Mechanics*, 125(11):1293–1297, 1999. doi: 10.1061/(ASCE)0733-9399(1999)125:11(1293).

[10] Z.Q. Cheng and R.C. Batra. Exact correspondence between eigenvalues of membranes and functionally graded simply supported polygonal plate. *Journal of Sound and Vibrations*, 229(4):879–895, 2000. doi: 10.1006/jsvi.1999.2525.

[11] J.N. Reddy and Z.Q. Cheng. Frequency correspondence between membranes and functionally graded spherical shallow shells of polygonal planform. *International Journal of Mechanical Sciences*, 44(5):967–985, 2002. doi: 10.1016/S0020-7403(02)00023-1.

[12] J. Yang and H.S. Shen. Dynamic response of initially stressed functionally graded rectangular thin plates. *Composite Structures*, 54(4):497–508, 2001. doi: 10.1016/S0263-8223(01)00122-2.

[13] J. Yang and H.S. Shen. Non-linear analysis of functionally graded plates under transverse and in-plane loads. *International Journal of Non-linear Mechanics*, 38(4):467–482, 2003. doi: 10.1016/S0020-7462(01)00070-1.

[14] S.S. Akavci, Mechanical behavior of functionally graded sandwich plates on elastic foundation. *Composites Part B: Egnineering*, 96:136–152, 2016. doi: 10.1016/j.compositesb.2016.04.035.

[15] M. Bouazza, Y. Kenouza, N. Benseddiq, and A.M. Zenkour. A two-variable simplified nth-higher-order theory for free vibration behavior of laminated plates. *Composite Structures*, 182:533–541, 2017. doi: 10.1016/ j.compstruct.2017.09.041.

[16] A.M. Zenkour and A.F. Radwan. Compressive study of functionally graded plates resting on Winkler–Pasternak foundations under various boundary conditions using hyperbolic shear deformation theory. *Archives of Civil and Mechanical Engineering*, 18(2):645–658, 2018. doi: 10.1016/j.acme.2017.10.003.

[17] A.M. Zenkour and A.F. Radwan. Free vibration analysis of multilayered composite and soft core sandwich plates resting on Winkler–Pasternak foundations. *Journal of Sandwich Structures and Materials*, 20(2):169–190, 2018. doi: 10.1177/1099636216644863.

[18] M. Touratier. An efficient standard plate theory. *International Journal of Engineering Science*, 29(8):901–916, 1991. doi: 10.1016/0020-7225(91)90165-Y.

[19] M. Stein. Nonlinear theory for plates and shells including the effects of transverse shearing. *AIAA Journal*, 24(9):1537–1544, 1986. doi: 10.2514/3.9477.

[20] J.N. Reddy. A general third-order nonlinear theory of plates with moderate thickness. *International Journal of Non-linear Mechanics*, 25(6):677–686, 1990. doi: 10.1016/0020-7462(90)90006-U.

[21] A.M. Zenkour. The refined sinusoidal theory for FGM plates on elastic foundations. *International Journal of Mechanical Sciences*, 51(11–12):869–880, 2009. doi: 10.1016/j.ijmecsci.2009.09.026.

[22] A.M. Zenkour. Hygro-thermo-mechanical effects on FGM plates resting on elastic foundations. *Composite Structures*, 93(1):234–238, 2010. doi: 10.1016/j.compstruct.2010.04.017.

[23] A.M. Zenkour. Buckling of fiber-reinforced viscoelastic composite plates using various plate theories. *Journal of Engineering Mathematics*, 50(1):75–93, 2004. doi: 10.1023/B:ENGI.0000042123.94111.35.

[24] A.M. Zenkour. On vibration of functionally graded plates according to a refined trigonometric plate theory. *International Journal of Structural Stability and Dynamics*, 5(2):279–297, 2005. doi: 10.1142/S0219455405001581.

[25] A.M. Zenkour. Generalized shear deformation theory for bending analysis of functionally graded plates. *Applied Mathematical Modelling*, 30(1):67–84, 2006. doi: 10.1016/j.apm.2005.03.009.

[26] A.M. Zenkour. Benchmark trigonometric and 3-D elasticity solutions for an exponentially graded thick rectangular plate. *Archive of Applied Mechanics*, 77(4):197–214, 2007. doi: 10.1007/s00419-006-0084-y.

[27] S.P. Timoshenko and W. Woinowsky-Krieger. Theory of Plates and Shells. New-York, NY: McGraw-Hill, 1970.

[28] K.Y. Lam, C.M. Wang, and X.Q. He. Canonical exact solution for Levy-plates on two parameter foundation using Green's functions. *Engineering Structures*, 22(4):364–378, 2000. doi: 10.1016/S0141-0296(98)00116-3.

[29] R. Buczkowski and W. Torbacki. Finite element modeling of thick plates on two-parameter elastic foundation. International *Journal for Numerical and Analytical Methods in Geomechanics*, 25(14):1409–1427, 2001. doi: 10.1002/nag.187.

[30] Z.Y. Huang, C.F. Lu, and W.Q. Chen. Benchmark solutions for functionally graded thick plates resting on Winkler-Pasternak elastic foundations. *Composite Structures*, 85(2):95–104, 2008. doi: 10.1016/ j.compstruct.2007.10.010.

[31] H-T. Thai and D.H. Choi. A refined plate theory for functionally graded plates resting on elastic foundation. *Composites Science and Technology*, 71(16):850–1858, 2011. doi: 10.1016/j.compscitech.2011.08.016.